

From Calibration to Astrophysics with the SMC SNR 1E0102.2-7219

Joseph M. DePasquale¹, Paul P. Plucinsky¹, Andrew P. Beardmore², Eric D. Miller³, A.M.T. Pollock⁴, Steve Sembay²

¹ Harvard Smithsonian Center for Astrophysics, 60 Garden Street, Cambridge, MA, USA 02138

² Department of Physics and Astronomy, University of Leicester, Leicester, LE1 7RH

³ MIT Kavli Institute for Astrophysics and Space Research, Cambridge, MA, 02139

⁴ European Space Astronomy Centre, Apartado 78, Villanueva del Canada, 28691, Madrid, Spain

Introduction

• The oxygen-rich supernova remnant (SNR) 1E0102-7219 has been extensively imaged throughout the Chandra X-ray Observatory's mission as a calibration source for ACIS.

• Through a comprehensive cross-calibration effort among several X-ray observatories, the spectrum of E0102 has been well modeled¹. Using the high-resolution grating instruments on-board XMM-Newton and the CXO, we have developed a consistent model which can be used to fit the lower resolution CCD.

• In addition to its effectiveness as a calibration tool, this model also provides a useful diagnostic tool for measuring spectral differences spatially within the remnant in an effort to identify the forward and reverse shock regions and to constrain ionization timescale and temperature measurements.

• Using 7 ACIS subarray observations taken between 2003 and 2009, together with a contour binning algorithm to define spectral extraction regions based on surface brightness, we explore spatial and temporal changes in both the physical structure and overall spectral properties of the remnant.



Figure 1: Chandra ACIS image of E0102 Red(200-750 eV); Green(800-1100 eV); Blue(1100-2000 eV)

Spatial Variations

• **Figure 5** to the right shows the region numbers corresponding to the spectra shown in the figures below.

• The spectral shape shows significant variation with position in the remnant, most notably in region 6 where the ratio of the Ne lines is significantly different.

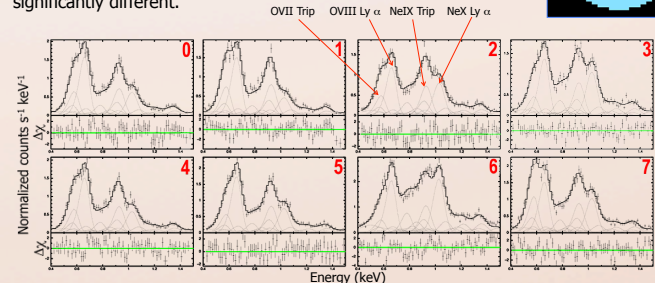
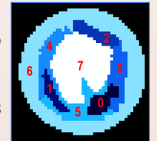


Figure 6: XSPEC fits to obsid 3545 for each of the contour bin regions.

• Fitted normalizations are multiplied by an effective area factor, and divided by the physical size of each region to create images in photons $s^{-1} \text{arcsec}^{-2}$ (see Figure 7)

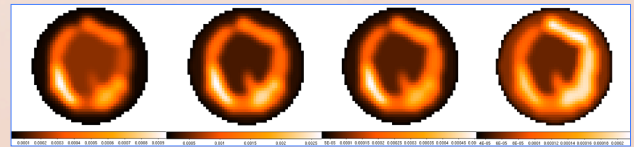


Figure 7: E0102 normalization images for OVII, OVIII, NeIX and NeX from obsid 3545

Data & Model

• Due to the effects of pileup on the full-frame ACIS observations, we focus this analysis on the 7 subarray observations listed in Table 1.

• Each dataset was processed using **CIAO & CALDB 4.1.2** including CTI and time dependent gain corrections.

OBSID	DATE	Yoffset	Duration(ks)
3545	2003-08-08	-1.0	8
6765	2006-03-19	-1.0	8
8365	2007-02-12	1.0	20
9694	2008-02-07	1.0	20
10654	2009-02-28	1.0	8
10655	2009-03-01	1.0	8
10656	2009-03-06	-1.0	8

Table 1: ACIS subarray observations of E0102.

• The model consists of two APEC "no line" components for the continuum along with two "tbabs" absorption components for galactic and SMC nH and 52 gaussians for the line emission between 0.2 and 2.0 keV¹. Figure 2 shows the model.

• In an effort to reduce the free parameters, the temperature and normalization of the continuum, and the absorption components are frozen to values derived from XMM MOS and pn fits. With the exception of O and Ne, all line energies, widths and normalizations are frozen to gratings derived values.

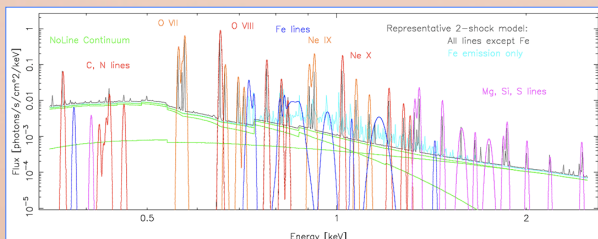


Figure 2: The line and continuum components of the E0102 model. The model was checked against a "vshock" model to insure that no bright lines in the band pass were missed.

Analysis Methods

• We make use of a contour binning algorithm to define spectral extraction regions based on a surface brightness variations in a smoothed image of E0102². Figure 3 shows an example of the 8 regions used for this analysis.

• Fits are done with **XSPEC v12.0** and line normalizations for the OVII triplet, OVIII Ly α , Ne IX triplet, and Ne X Ly α lines are collected.

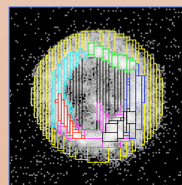
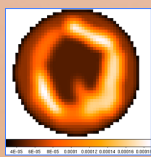


Figure 3: Spectral extraction regions defined by contour binning.

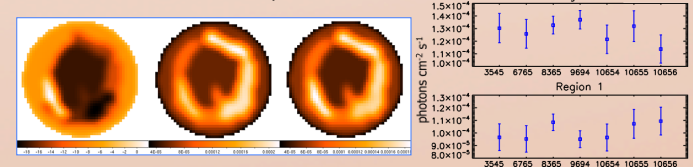


• Line normalization values, together with the binning map defined by the algorithm can be used to "paint" images of the remnant in O and Ne normalization. These images can be further processed to explore temporal variations.

Figure 4: An image of E0102 from obsid 10656 in Ne X Ly α normalization.

Temporal Variations

• Using the adjusted normalization images, we calculate percentage difference maps between observations. Here we consider an example of comparing the earliest and latest observations in the Ne 10 Ly α normalization:



Figures 8 & 9: The percentage difference in normalization of Ne X is shown on the left, with the original normalization images from obsids 3545 and 10656 to compare. The largest changes are a 20% drop in normalization in region 0 and a 2% increase at region 1. Given the uncertainties in the normalization measurements as shown in the plot on the right, it is not possible to constrain this temporal change. Within errors, the Ne X normalization is consistent throughout the 7 observations considered. This result applies to the O VII, O VIII, and Ne IX lines as well.

Conclusions

• A spatial/temporal analysis of the SMC SNR E0102 was presented using contour binning to define spectral extraction regions based on a surface brightness variations.

• Using the spectacular resolution of Chandra, we see a great diversity in the ratios of the Oxygen and Neon lines extracted from various regions of the remnant.

• Within 90% confidence limits, we do not see evidence for any spectral variations over time within this 6 year sample of data.

• Future work on this project will include exploring more of the parameter space within the model by allowing the underlying continuum temperature to vary. We also intend to account for the effects of pileup in the full frame data and make use of the larger volume of available data.

References & Acknowledgements

1. Plucinsky, P. et al. arXiv:0807.2176v1 [astro-ph]

2. Sanders, J., MNRAS, 371, 829-842 (2006)

This work was supported by NASA contract NAS8-39073.